Hydrolysis of Monodisperse Phosphatidylcholines by Phospholipase A_2 Occurs on Vessel Walls and Air Bubbles†

Bao-Zhu Yu,‡ Otto G. Berg,§ and Mahendra Kumar Jain*,‡

Department of Chemistry and Biochemistry, University of Delaware, Newark, Delaware 19716, and Department of Molecular Evolution, Uppsala University Evolutionary Biology Centre, Uppsala, Sweden

Received January 26, 1999; Revised Manuscript Received June 16, 1999

ABSTRACT: Hydrolysis of monodisperse short chain phosphatidylcholines, far below their critical micelle concentration, by phospholipase A_2 (PLA2) and other interfacial enzymes is characterized. Results show that virtually all the observed hydrolysis by pancreatic and human inflammatory PLA2 occurs on surfaces of the reaction vessel or air bubbles. Conditions to eliminate such extraneous contributions at low substrate concentrations are established. Premicellar aggregates are apparently formed near the critical micelle concentration. The observation window at low substrate concentrations is used to obtain an upper limit estimate of the rate of hydrolysis through the monodisperse Michaelis complex. A limit estimate of <0.1 s^{-1} is obtained for the hydrolysis of monodisperse substrates by pig pancreatic phospholipase A_2. These results show that the observed rate of hydrolysis of dihexanoyl- and diheptanoylphosphatidylcholines with pig pancreatic phospholipase A_2 through the monomer path is insignificant compared to the rate of >1000 s^{-1} seen at the saturating levels of the micellar substrate. These protocols should be useful for evaluating reactions catalyzed at vessel walls. Implications of these results for assays and models of interfacial activation of pancreatic PLA2 are discussed.

Interfacial enzymes have evolved to catalyze reactions on interfaces because that is where their substrates are to be found. For example, hydrolysis catalyzed by phospholipase A_2 (PLA2)[1] on anionic bilayer interfaces occurs with high processivity; i.e., the enzyme does not dislodge during or between the turnover cycles at the interface (*1*−*3*). The observed rate of hydrolysis of the short chain phosphatidylcholines by pancreatic PLA2 increases significantly above the cmc (*4*, *5*). Under suitably constrained (*3*) or optimized conditions of rapid substrate replenishment (*6*), the primary kinetic parameters for the hydrolysis at the micellar interface are remarkably similar to those for the hydrolysis in the highly processive scooting mode at the vesicle interface (*3*, *7*). Having established a kinetic basis for enzymology at micellar and vesicle interfaces (Scheme 1), we have shown that the substrate binding to the active site is enhanced by the binding of PLA2 to the interface (*8*), and that the anionic charge at the interface activates the chemical step (*6*). This analysis of interfacial turnover and activation, in terms of the primary rate and equilibrium parameters of kinetic Scheme 1, paves the way for evaluating the structural basis for the interfacial enzymology of PLA2.

Scheme 1: Primary Rate and Equilibrium Parameters at the Interface (marked with an asterisk) and the Aqueous Phase (without an asterisk) Defined According to Standard Nomenclature Based on the Michaelis Formalism Adopted for Interfacial Enzymology[a]

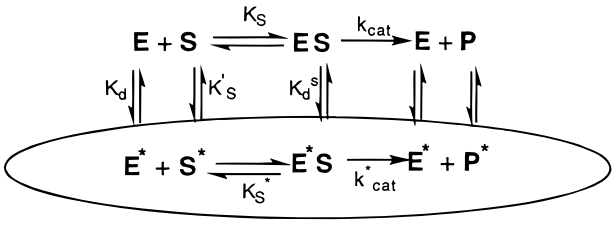

[a] Enzyme-mediated catalytic turnover can occur at the interface (through E* and E*S) as well as in the aqueous phase through the decomposition of a solitary ES complex in the bulk aqueous phase with k_{cat} and k_{cat}* being the rate constants for decomposition of ES and E*S, respectively. For details, see ref *6*.

Structural information about proteins at interfaces is difficult to obtain with the available methods. Therefore, the behavior of PLA2 in the aqueous phase is a functionally relevant reference state for a correlation of the crystallographic and solution structure to its catalytically relevant interfacial structure. In accord with Scheme 1, we address the question of whether PLA2 hydrolyzes a monodisperse substrate through the turnover cycle in the aqueous phase via a monodisperse ES. Typically, this is not a concern because the monomer concentration of naturally occurring phospholipids in the aqueous phase, in equilibrium with bilayers and mixed micelles, is less than 100 pM. However,

† This work was supported by the U.S. Public Health Service (Grant GM29703 to M.K.J.) and the Swedish Natural Science Research Council (to O.G.B.).

* Corresponding author. Phone: (302) 831-2968. Fax: (302) 831-6335. E-mail: mkjain@udel.edu.

‡ University of Delaware.

§ Uppsala University Evolutionary Biology Centre.

[1] Abbreviations: cmc, critical micelle concentration; DC_nPC, 1,2-diacylglycero-*sn*-3-phosphocholine with *n* carbons in each acyl chain; DC_nPC-ether, 1,2-dialkylglycero-*sn*-3-phosphocholine with *n* carbons in each acyl chain; DMPM, 1,2-dimyristoylglycero-*sn*-3-phosphomethanol; DTNB, dithiobis(dinitrobenzoic acid); GCAT, lipase/acyltransferase from *Aeromonas hydrophila*; MJ33, 1-hexadecyl-3-(trifluoroethyl)-*rac*-glycero-2-phosphomethanol; PLA2, phospholipase A_2 from pig pancreas unless noted otherwise; SNAFL, ammonium salt of calcein.

10.1021/bi990194z CCC: $18.00
Published on Web 07/16/1999

for short chain phospholipids, the monomer substrate concentration in the aqueous phase can be in the millimolar range. The rates of hydrolysis of short chain phosphatidylcholines below the cmc are considerably slower than the saturating rate above the cmc (*4*, *5*). This observation has been the basis for much of the discussion about interfacial activation during the past several decades with the interpretation that the observed premicellar rate is due to the hydrolysis of a monodisperse substrate via the monodisperse ES Michaelis complex (Scheme 1).

The turnover through the monomer path bears on fundamental issues of interfacial catalysis, yet hydrolysis of monodisperse substrates by PLA2, for example, the short chain phospholipids below the cmc, remains an enigma. As it turns out, this interpretation as a reaction via the monomer parth (*4*, *5*) is inconsistent with the inhibitor binding (*9*, *10*), as well as the kinetic and spectroscopic results (*11*) where in the presence of a monodisperse substrate and inhibitor the pig PLA2 behaves as if it is at the interface. To reconcile this apparent contradiction, we have systematically examined the hydrolysis of monodisperse short chain phosphatidylcholines by pig pancreatic PLA2. Results show that virtually all the observed hydrolysis at low concentrations of a monodisperse substrate occurs on surfaces of walls of the reaction container and the surface of air bubbles formed during vigorous stirring and shaking. If such extraneous factors are eliminated, the rate of hydrolysis through the monodisperse ES complex is immeasurably small ($<0.1\ s^{-1}$).

EXPERIMENTAL PROCEDURES

Sources of reagents and most analytical and experimental protocols have been described previously (*3*, *6*, *7*), and only salient details are given below. The pH indicator dyes, pyranine and SNAFL, were purchased form Molecular Probes. DC_nPCs and the corresponding ethers (custom synthesis) were from Avanti Polar Lipids. MJ33, DMPM (*12*), and DC_{14}PC-ether (*13*) were synthesized. Dithio-DC_6-PC was kindly provided by S. Hendrickson. PLA2 from *Naja melanoleuca* (*14*) and GCAT (*15*) were obtained as described previously. All other reagents were analytical grade. Uncertainty in the measured values is 15%.

Kinetic Protocols. Kinetics of the proton release by the PLA2-catalyzed hydrolysis was measured by three methods in 1 mM $CaCl_2$ and 1 mM NaCl at 25 °C in a nitrogen-purged atmosphere.

(a) The first method involved analysis in mechanically stirred solutions in polypropylene cups by the pH-stat method using a Brinkman (Metrohm) or a Radiometer titrator with 3 mM NaOH titrant in the buret (*1*, *6*). The contribution of the reaction at walls and air bubbles cannot be controlled in this assay.

(b) Virtually identical conditions were used for monitoring the hydrolysis of dithio-DC_6PC in unstirred quartz cuvettes containing 10 mM Tris at pH 7.5, except that the thiol product was quantified by reaction with dithiobis(dinitrobenzoic acid) (DTNB). The contribution of the reaction on the air bubbles becomes apparent after vigorous shaking of the cuvette.

(c) Reaction progress was also monitored as the fluorescence change from pyranine (excitation and emission at 460 and 530 nm, respectively) or SNAFL (excitation and emission at 538 and 620 nm, respectively) in magnetically stirred or unstirred polystyrene or quartz cuvettes containing 0.2 mM Tris at pH 7.1 in a nitrogen-purged cuvette compartment of a SLM AB2 spectrofluorimeter. Acidification decreases the fluorescence emission intensity from both the dyes, and the conditions were chosen such that the decrease was linearly proportional to the concentration of added protons. Standard quartz or polystyrene plastic cuvettes (Fisher catalog no. 14-386-20) were used as indicated. A cuvette spin-bar (9 mm diameter and 8 mm height) coated with Teflon (Bell Art Products) was used in the fluorescence cuvettes.

Stock dispersions of DC_nPC or other lipids in water were added to the reaction mixture and equilibrated in the cuvette compartment continuously purged with nitrogen. All subsequent additions were made with a microsyringe through a pinhole in the lid of the compartment above the reaction cuvette. Typical background drift rates were 2 pmol/s, and necessary corrections are made in the calculated results. The reaction was typically initiated by the addition of the enzyme (0.1 to >100 pmol), depending on the observed slope. In stirred solutions, hydrolysis commenced in less than 3 s after the addition of enzyme if the reaction occurs in the bulk phase. Inhibitor and other components, if present in the reaction mixture, gave identical results whether they were added before or after initiating the reaction. Controls also showed that the sequence of the addition of substrate or PLA2 does not noticeably affect the observed rates. Initial rates are expressed as observed rates per second with an estimated uncertainty of 20% at the lower end and 10% for rates above $1\ s^{-1}$.

The amount of proton or product release under specific reaction conditions in the fluorescence assay was calculated from calibration curves obtained with added heptanoic acid. Such curves also provided the linear response range. Results in the presence of 4 M NaCl are corrected for a small change in the titration efficiency. The fidelity of the dye assay was also ascertained by comparing the reaction progress with DMPM in the scooting mode on anionic phospholipid vesicles without (*1*) and with the polymyxin B-induced rapid phospholipid exchange between vesicles (*2*). These and other controls with micellar substrates (*6*) showed that the absolute rates obtained by the three methods for monitoring the hydrolysis were within a 30% range under comparable conditions. Both the pH-indicator dyes gave virtually identical results with monodisperse substrates; however, only the results with SNAFL are given. Significant departures in the emission from pyranine were observed in the presence of a micellar substrate, as if pyranine has significant affinity for the lipid interface.

RESULTS

In this paper, we show a dramatic dependence of the kinetics of PLA2-catalyzed hydrolysis of monodisperse DC_6-PC or DC_7PC on the presence of extraneous interfaces, which presumably provide sites for the binding of the enzyme and the substrate. A demonstration of the effect of air bubbles and the cuvette surface on the observed rate of hydrolysis of dithio-DC_6PC, below its cmc of 2 mM, is shown in Figure 1. The reaction begins immediately after the addition of

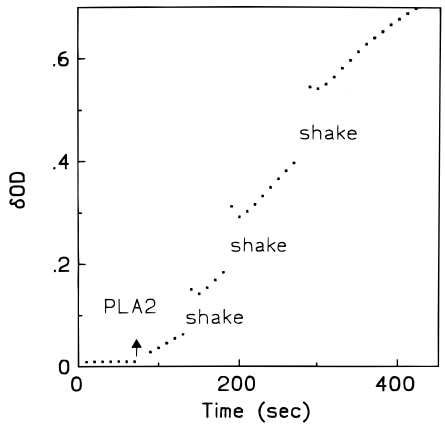

FIGURE 1: Time course of hydrolysis of 0.5 mM dithio-DC_6PC by 2.5 μg of pig PLA2 monitored as the OD change at 412 nm for the product of the thiolysophospholipid with DTNB. A burst of OD change is seen when the cuvette is intermittently shaken.

PLA2. On the basis of the total amount of enzyme in the reaction mixture, the observed rate in this spectroscopic assay is about 0.1 s^{-1} under unstirred conditions. A 10-fold higher rate, about 1.2 s^{-1}, measured in stirred and vigorously shaken cuvettes is comparable to that seen in the vigorously stirred pH-stat assay (*6*). Remarkably, a burst of the absorbance change is seen as the contents of the cuvette are shaken. The burst is seen only in the presence of the enzyme and the substrate. The amplitude of the burst depends on the time lapse between the mixing to bring the products formed on the walls into the beam path. A contribution of reactions on the air−water surface of bubbles formed by shaking is also indicated by the amplitude of the burst, which increases if the cuvette is shaken more vigorously or for a longer period of time. Although such variables are difficult to quantify for detailed analysis, their contributions are virtually completely eliminated in the fluorescence assay protocol described below.

Hydrolysis without the Reaction on the Cuvette Walls. In fluorescence measurements, the observation window is effectively shielded from the contribution of the reaction on the cuvette walls. As shown in Figure 2, walls in the path of the excitation and emission beams are orthogonal such that the observation volume, where the excitation and emission paths intersect, is well separated from the walls. This setup at small beam widths limits the ability to excite and to detect emission from the same walls. In unstirred solutions, the product from any of the walls will have to diffuse through layers of the bulk aqueous phase to come into the observation window. As modeled in Appendix, such a diffusion delay is expected to be on the order of several minutes.

The contribution of the diffusion layer to reaction progress is shown in Figure 3A. The reaction begins after PLA2 is added to the stirred solution, and a small delay is seen in the plastic cuvette. In both cases, the apparent rate decreases dramatically as soon as stirring is ceased. Note that as stirring is begun again, in both cases a burst of the fluorescence decrease is followed by a sustained decrease with a slope that is virtually identical to that seen before the stirring was ceased. The burst is due to the fact that in unstirred solutions the reaction continues on the container walls without a significant contribution in the observation window. When the contents were stirred, all the product accumulated near

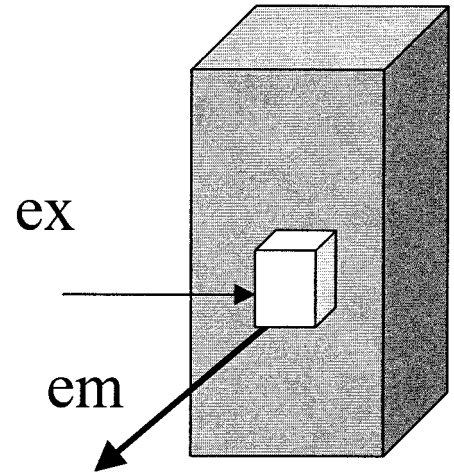

FIGURE 2: Geometry of the beam path and the unstirred layer in the cuvette (lightly shaded area) for the measurement of the fluorescence change under the conditions for the results depicted in Figure 3 and modeled in the Appendix. The observation volume in the center (hatched) is isolated from the cuvette walls by an unstirred layer if the bulk solution is not stirred.

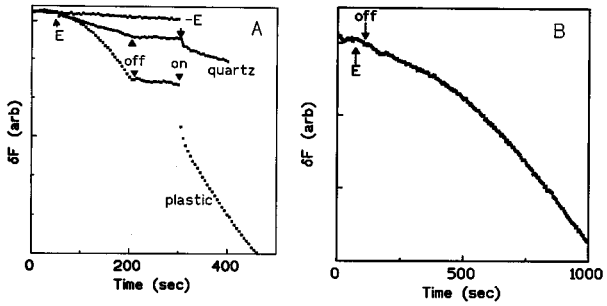

FIGURE 3: (A) Time course of the hydrolysis of 0.438 mM DC_6-PC by 2.6 μg of pig PLA2 monitored as the fluorescence change due to a change in pH. From the top, the traces correspond to a reaction mixture without the enzyme and the reaction mixture with enzyme in a quartz or plastic cuvette. The rate of fluorescence change decreases significantly when the reaction mixture is not stirred. (B) Time course of the hydrolysis of unstirred 0.438 mM DC_6PC by 2.6 μg of pig PLA2 monitored as described for panel A. Essentially the same time course is modeled in the Appendix.

the wall in the unstirred layer mixes with bulk solution. Note that the slope after the burst is the same as before stirring was ceased, and that the amplitude of the burst at short times increases with the duration for which the stirring is ceased (not shown). Since reaction progress continues after the burst at roughly the extrapolated levels from before, it is concluded that hydrolysis continues at roughly the same rate also during the time that stirring is ceased. The conclusion that the burst and the stirred rate are due to the reaction at the cuvette wall is consistent with the observation that the apparent rate of reaction by both of these criteria is significantly higher on the plastic cuvette than on the quartz cuvette (Figure 3A). We do not know the reason for this difference, although it is expected if more enzyme is bound, or the activity is higher on the plastic cuvette.

The steady state rate of hydrolysis, or the burst on beginning the stirring, was not seen in reaction mixtures where one of the components needed for the reaction is not included. Such controls showed that the stirred rate is not seen in the absence of calcium, the catalytic cofactor, or in the presence of a competitive inhibitor, MJ33. In unstirred

solutions, the steady state slope remains barely above the background in both types of cuvettes. Note that the experimental conditions chosen for the experiment whose results are depicted in Figure 3A, and for virtually all other results described in this paper, are such that the fluorescence change is a linear function of the amount of the short chain fatty acid produced during the course of the reaction. As described in Experimental Procedures, the calibration curves for the fluorescence response under the assay conditions were generated with heptanoic acid. Only the concentration range that gave a linear fluorescence response was used for the measurement of PLA2-catalyzed hydrolysis.

The contribution from the reaction on the walls, limited by the diffusion through the unstirred layer, would be significant only after longer periods of time in the fluorescence observation window. The thickness of the unstirred layer in our cuvette system is estimated to be 0.24 cm. As developed in the Appendix, the diffusion delay through an unstirred layer of 0.24 cm is expected to be about 10 min. The experimental curve in Figure 3B is in good accord with this calculation. The main purpose of these calculations is to show that the observed time delay is consistent with the time required for the product (protons) from the walls to diffuse into the path of the observation beam. If the hydrolysis on the walls continues for some period of time, the overall rates could soon become limited also by the replenishment of substrate from solution, unless most of the substrate is at the walls already from the beginning. In this case, there can be no steady state and the overall rate would decline long before the total substrate is hydrolyzed. This process can be affected in a variety of manner by details of the product diffusion. Hydrolysis will also be affected by product inhibition as the product accumulates in the wall region. At present, we do not have sufficient information about the initial substrate distribution on the cuvette walls or product inhibition, to predict the overall kinetics. However, data depicted in Figure 3A show that during the 100 s that stirring is ceased hydrolysis at the walls continues at the same rate. This suggests that substrate replenishment and product inhibition do not play any role during this time, as is assumed to be the case for the calculations.

Independent controls were carried out to ascertain the fidelity of the proton release assayed with pyranine and SNAFL. Comparisons under a variety of conditions showed that results with both dyes are identical to those obtained with the pH-stat assay. Considerable anomaly is observed under the conditions where the response profile and partitioning of pyranine in lipid dispersions change with pH. For quantitative comparisons, we describe results only with SNAFL. Such controls showed that in the scooting mode hydrolysis of only the enzyme containing DMPM vesicles occurs as predicted by the Poisson distribution relationship (*1*), and hydrolysis of excess vesicles occurs in the presence of polymyxin B (*3*). Similarly, enhanced hydrolysis of micellar DC_nPC is seen above the cmc as described later, as is the fact that the rate of hydrolysis of micellar substrate increases up to 100-fold in 4 M NaCl (*6*). Such comparisons suggest that the fluorescence change characterized in panels A and B of Figure 3 reflects the events associated with PLA2-catalyzed hydrolysis at the cuvette walls. Since higher activity is seen on the surface of the polystyrene cuvette, it appears that the enhanced rate is driven by the hydrophobic effect. This also accounts for the lower rates seen in the quartz cuvette in the spectroscopic assay, and for the higher rates seen in polypropylene cups used for pH-stat titration (Table 1). Addition of cation exchange beads or carboxymethyl cellulose powder did not induce a noticeable increase in the stirred rate, which suggested that ionic interactions at extraneous surfaces are probably not responsible for the effects.

Table 1: Rate of Hydrolysis of 0.1 mM DC_7PC by Pig PLA2

conditions	rate (s^{-1})	conditions	rate (s^{-1})
pH-stat	4.5	stirred plastic cuvette	2.5
stirred quartz cuvette	0.5	unstirred plastic cuvette	0.04
unstirred qartz cuvette	0.04		

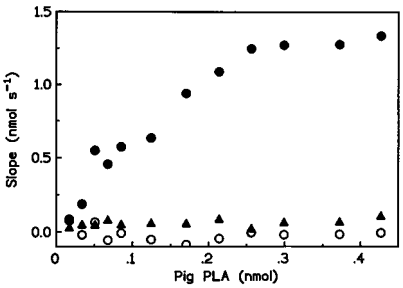

FIGURE 4: Dependence of the slope of the fluorescence change in a plastic cuvette as a function of the added amount of pig PLA2 monitored in 0.2 mM Tris, 5 mM $CaCl_2$, and 1 mM NaCl for the stirred (●) and unstirred reaction mixtures (▲) containing 0.44 mM DC_6PC. The background drift rate (○) in the absence of added enzyme is also shown.

Dependence of the Apparent Stirred Rate on the Amount of PLA2 Is Saturable. A consequence of the reaction at the walls of the vessel is that the surface could saturate with absorbed PLA2. As shown in Figure 4, the slope for the stirred reaction increases steeply at low pig PLA2 concentrations and then reaches an apparent maximum. On the other hand, the slope in unstirred solution is only slightly above the background drift. The slope for the unstirred reaction barely changes with the amount of PLA2, as is also the case at saturating levels of the stirred slope. Above 0.2 nmol, the excess enzyme apparently does not contribute to the observed hydrolysis. If the reaction occurs only on the walls, with the stirred cuvette and spin-bar surface of about 10 cm^2 covered by 0.2 nmol of PLA2, one enzyme occupies about 1300 $Å^2$. On a perfectly flat surface, this would be a reasonably close-packed layer.

As summarized in Table 2, a dependence of the observed rate on stirring is seen with several other phospholipases. On the basis of the slope of the initial region of the plot in Figure 4, the apparent rate of hydrolysis by pig PLA2 in a stirred solution is about 2.5 s^{-1} in 100 μM DC_7PC or 5 s^{-1} in 0.4 mM DC_6PC. The stirred rate calculated from the PLA2 concentration dependence in the saturating region is <0.1 s^{-1}, and it is comparable to that estimated from the slope of the enzyme concentration dependence under the unstirred conditions. A maximum of the stirred rate was also observed with increasing concentrations of certain other lipases (Table 2). For example, the stirred and unstirred rates are significantly different for GCAT and for PLA2 from venom of the *N. melanoleuca* DEII isozyme. For the 14 kDa *Naja* enzyme, saturation of the slope occurs at about 0.15 nmol, whereas for the 34 kDa GCAT, it occurs at about 0.08 nmol. The

Table 2: Upper Limit Estimate of the Rate of Hydrolysis of DC_6PC (0.438 mM) in Unstirred and Stirred Cuvettes

enzyme		rate[a] (s^{-1}) unstirred	stirred
pig	quartz	0.06	0.2
	plastic	0.07	5.3
human type II	plastic	<0.005	0.1
Naja (DE2)	plastic	0.03	10.4
bee venom	plastic	34	40
GCAT	plastic	0.5	29

[a] Rates (standard deviation of ±15%) were measured in 1 mM NaCl, 5 mM $CaCl_2$, and 0.2 mM Tris at pH 7.1 with 0.438 mM DC_6PC at several enzyme concentrations (cf. Figure 4). The unstirred rates are based on the slope of the line for the enzyme concentration dependence.

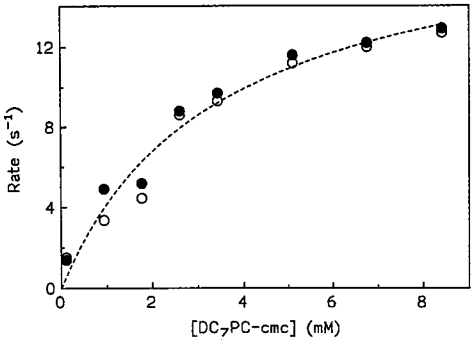

FIGURE 5: Dependence of the rate of hydrolysis of micellar DC_7PC by PLA2 for the stirred (●) and unstirred (○) reaction mixtures in plastic cuvettes. The other conditions were as described in the legend of Figure 4.

unstirred rates with type II human PLA2 are also barely above the background level, and a modest increase is seen on stirring. On the other hand, bee venom PLA2 exhibits a considerably higher unstirred rate, and the increase on stirring is also modest. Either the bee venom PLA2 hydrolyzes the monodisperse substrate, or the unstirred rate could be due to the formation of premicellar aggregates which remain in the bulk aqueous phase (*17*). Such alternatives cannot be resolved yet.

Stirring Does Not Change the Rate above the CMC. Results so far suggest that virtually all the hydrolysis of monodisperse short chain phosphatidylcholines is due to the pig pancreatic PLA2-catalyzed reaction on walls of the reaction vessel. The contribution of the extraneous surfaces is minimized with micellar substrates. As shown in Figure 5, the rate of hydrolysis increases with micellar DC_7PC concentration, and the stirred and unstirred rates are virtually the same. Indeed, the dependence of the rate of hydrolysis on the micellar DC_7PC concentration in the absence of added NaCl gives the following apparent rate parameters obtained from the hyperbolic fit shown in Figure 5: $K_M^{app} = 3.0$ mM and $V_M^{app} = 18\ s^{-1}$. These values compare favorably with the values of 2.3 mM and 16 s^{-1}, respectively, obtained with the pH-stat titration protocol under the same conditions (*6*). This is expected because above the cmc the rate is dominated by the partitioning of the enzyme on micelles and the interfacial catalytic turnover occurs at the micellar interface with a substrate replenishment on the time scale of the catalytic turnover time.

Conditions for Minimizing Adsorbed PLA2. Our observations with the adsorption of PLA2 on cuvette surfaces and

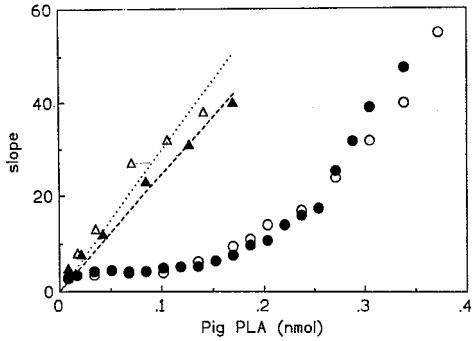

FIGURE 6: Effect of increasing the amount of added PLA2, in a stock solution stored in the plastic cuvette, on the transferred activity determined in a separate cuvette by using 1-palmitoyl-2-pyrenedecanoylphosphatidylmethanol substrate (*17*). The conditions in the stock cuvette for changing the amount of added enzyme were identical to those described in the legend of Figure 4, but without (○) or with added 0.2 mM DC_6PC-ether (●). For the controls without (△) and with the ether (▲), the stock solution at the same concentration was prepared in borosilicate glass minitubes (Kimbell) where the extent of adsorption is considerably lower.

air bubbles raise a generic concern about the storage, transfer, and assay conditions for PLA2. We explored conditions under which the enzyme present in a stock solution in a polystyrene cuvette becomes available for transfer to a separate cuvette for an assay which is not affected by adsorption. In this scooting mode assay, the affinity of PLA2 for the anionic 1-palmitoyl-2-pyrenedecanoylphosphatodylmethanol vesicle interface is high and virtually all the enzyme remains at the vesicle interface even when all the substrate is hydrolyzed (*3*, *16*, *17*). As shown in Figure 6, about 0.2 nmol of PLA2 cannot be transferred from a plastic cuvette, and only the excess PLA2 is transferable. Note that the amount of PLA2 that is not transferable is comparable to the absorbed amount that was available for the surface reaction depicted in Figure 4. This is because identical conditions are used in these two complementary sets of experiments, although the amount of enzyme in the supernatant is determined by two different criteria. Even the presence of 0.2 mM DC_6PC-ether, more than 10 times below the cmc, in the stock solution does not make more enzyme transferable. On the other hand, virtually all the enzyme from the stock solution in borosilicate tubes under the same conditions can be transferred to the assay mixture. Together, the complementary results depicted in Figures 4 and 6 show that PLA2 adsorbed on the cuvette walls is responsible for the stirred rate.

The effect of added γ-globulin on the amount of transferable PLA2 from a glass storage vial is shown in Figure 7. Under these conditions, a maximum of 80% PLA2 in the stock solution can be transferred to the assay mixture at saturating globulin levels. The comparisons in Figure 7 show that even in the presence of 15 mM DC_6PC-ether and a saturating amount of globulin the transferable fraction of the total enzyme did not reach 100% unless 4 M NaCl was also added to the stock solution. Independent experiments also showed that 4 M NaCl alone did not increase the transferability of the adsorbed enzyme.

We investigated the conditions under which pig PLA2 bound to the container walls is completely transferable. As shown in Figure 8, the transferable fraction of the total pig PLA2 from the plastic cuvette decreases with increasing

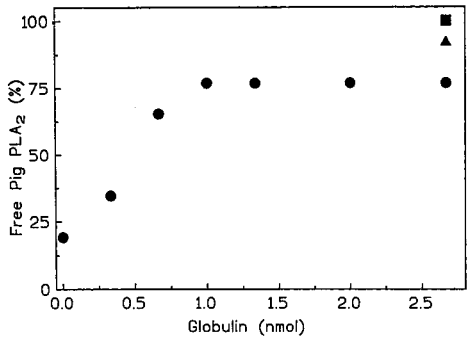

FIGURE 7: Effect of added γ-globulin on the amount of transferable enzyme from a stock solution in a glass vial (●). Conditions for the incubation of 0.12 nmol of pig PLA2 were identical to those described in the legend of Figure 4. The effect of added 15 mM DC_6PC-ether alone (▲) or with 4 M NaCl (■) is an increase in the fraction of transferable enzyme closer to 100% of the enzyme originally added to the container.

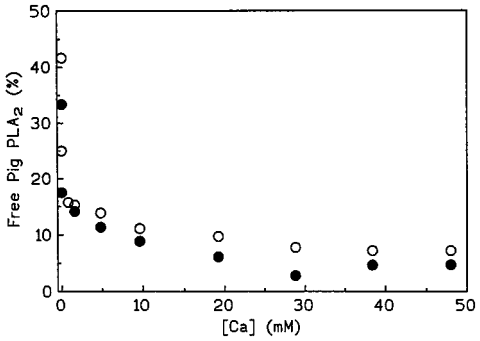

FIGURE 8: Effect of the calcium concentration on the fraction of the transferable enzyme in the stock solution in a plastic cuvette without (○) or with (●) 0.2 mM DC_6PC-ether. Conditions for the incubation of 0.12 nmol of pig PLA2 without added globulin were identical to those described in the legend of Figure 4.

calcium concentrations. The overall effect on the nontransferability appears to have two components, which may have an interesting kinetic consequence. As more enzyme is adsorbed, the stirred rate will increase with increasing calcium concentrations. This effect is of course in addition to the direct effect of calcium on the catalytic turnover (*16*). The two apparent dissociation constants from the results depicted in Figure 8 are 0.3 and 5 mM, as also reported under the kinetic conditions with weak interfaces (*5*). Note that calcium has little effect on the binding of PLA2 to the phospholipid interface; therefore, the apparent effects of calcium on the adsorption on cuvette walls must involve additional considerations.

Optimum conditions for the desorption of pig PLA2 bound to the plastic cuvette walls are provided by results shown in Figure 9. The transferable PLA2 activity increases with increasing DC_6PC-ether concentrations. In the absence of added NaCl, the inflection corresponds to the cmc of the ether, and 95% of the enzyme can be transferred at >15 mM. In the presence of 4 M NaCl, virtually all the bound enzyme becomes transferable at <2 mM DC_6PC-ether. Recall that the cmc of the ether is 0.5 mM in 4 M NaCl, which also increases the affinity of PLA2 for the zwitterionic interface (*6*). In short, PLA2 bound to container walls can be totally competed out with DC_6PC-ether at 4 M NaCl for transfer. These conditions are well suited for making dilute stock solutions of PLA2 because additional 1000-fold

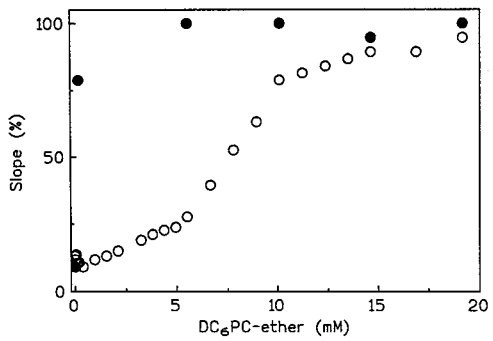

FIGURE 9: Effect of DC_6PC-ether concentration on the fraction of the transferable enzyme in the stock solution in a plastic cuvette without (○) or with (●) 4 M NaCl. Conditions for the incubation of 0.12 nmol of pig PLA2 were identical to those described in the legend of Figure 4.

dilution of NaCl and DC_6PC in the assay mixtures will have little adverse kinetic effect.

DISCUSSION

The Michaelis−Menten kinetic paradigm is adopted for interfacial catalysis in Scheme 1 with two parallel paths for catalytic turnover, one through the interface and the other in the aqueous phase. The relative magnitudes of the primary kinetic parameters for the two paths constitute the basis for interfacial activation (*6*, *8*). Lipolytic enzymes have evolved to work at interfaces because that is where their natural substrates are found. Interfacial catalysis assessed in the scooting mode (*1*, *3*, *7*) or under the fast exchange conditions (*6*) provides the only conditions for determining the interfacial kinetic parameters. The results of this study clearly show that no useful mechanistic information for PLA2 can be obtained from assays with monodisperse substrates; however, a limit estimate of the turnover through the monomer path is theoretically interesting.

Under optimum conditions, the interfacial catalytic turnover by pig PLA2 with DC_7PC micelles is >500 s^{-1}, and the measured rate with DC_6 PC is about 250 s^{-1} (*6*). Our estimate for the rate of hydrolysis of monodisperse short chain phosphatidylcholines is significantly less than 0.1 s^{-1}. This limit estimate for the monomer hydrolysis by PLA2 is 10−100-fold smaller than that reported previously. Virtually all of the difference can be attributed to the contribution from the extraneous reaction on surfaces of container walls and air bubbles. Our assay conditions are also chosen to minimize possible contributions from premicellar aggregates of the enzyme with substrate amphiphiles (*11*). Analysis of anomalous effects, associated with the possible formation of the premicellar aggregates of PLA2 at substrate concentrations closer to the cmc, will require additional studies.

It has been reported that monodisperse substrate mimics bind to the active site of PLA2. As is the case at the interface, the mimic binding to the active site of PLA2 in aqueous phase has an obligatory requirement for calcium (*9*, *10*). In addition, catalytic His-48 is not alkylated in such complexes (*6*, *8*). For the interpretation of these results, we assumed that the mimic does not promote the formation of the premicellar aggregates, which gives an apparent dissociation constant for DC_7PC-ether of 0.08 mM. If K_M for the monomer path is also in this range, the upper limit estimate for k_{cat} via monodisperse ES will be <0.5 s^{-1} for DC_7PC. If

a premicellar aggregate is formed under the conditions of the alkylation assay (*16*), the stability of monodisperse ES will be even lower. In short, we believe that if a monodisperse substrate binds to the active site of PLA2 in solution, the monodisperse ES complex is virtually completely catalytically impaired.

Impaired hydrolysis of short chain phosphatidylcholines through the monomer path may have its origin in factors that control the chemical step at the interface. Pig PLA2 is activated by the anionic charge at the interface. For example, in the absence of an additive on DC_7PC micelles, k_{cat}* is less than 20 s^{-1}, compared to a value of about 1000 s^{-1} at the anionic interfaces or in the presence of 4 M NaCl (*6*). We cannot yet rule out the possibility that the steady-state accumulation of the anionic products of hydrolysis is responsible for building an anionic charge even on these DC_7-PC zwitterionic micelles at low salt concentrations. If so, it would imply that most, if not all, catalytic activity of pig PLA2 is expressed only at the anionic interface. Site-directed mutagenesis studies suggest that the k_{cat}* activation by the anionic charge at the interface is due to interaction of K56 and K53 on the interfacial recognition surface of PLA2 away from the active site (*18*). We surmise that PLA2 will remain k_{cat}*-impaired in the absence of such charge interactions in monomer ES in the aqueous phase. We are investigating consequences of such possibilities.

Implications of Catalysis on Extraneous Surfaces. Our results showing adsorption of PLA2 on vessel walls raise doubt about the fidelity of many of the commonly used assay conditions. Such concerns are also relevant for the enzymology on monolayers of medium chain phospholipids at the air−water interface. Typically, the monolayer area is comparable to the trough area, and it has long been appreciated that only a small fraction of PLA2 added to the aqueous phase binds to the monolayer (*19*). In conjunction with the inability to ascertain the steady-state condition due to diffusion though the unstirred aqueous layer (*20*), the concern about a possible reaction on hydrophobic walls of a Teflon trough needs be addressed.

Synovial and pancreatic PLA2 have low affinities and low k_{cat}* values on phosphatidylcholine vesicles. This raises a warning flag about the fidelity of assays in which a small amount of substrate with a weakly binding interface is used, as is typically the case with radiolabeled or certain fluorescent substrates where the background counts have to be kept low. The problem of adsorption on extraneous surfaces is expected to be particularly acute in assays with biological fluids containing a small amount of interfacial enzyme shaken in a plastic tube. Only when the surface is saturated with the enzyme can one at best hope to obtain a relative measure of activity without knowledge of the amount of enzyme at the substrate interface. The lag period seen under these conditions is followed by a burst of activity after a critical mole fraction of the products has accumulated (*20*, *21*). The magnitude of the lag phase depends not only on the variables that control the initial binding of PLA2 to the interface but also on the competitive binding to the extraneous surfaces. Since such variables cannot be readily controlled, the lag period in this kinetic assay cannot be used as a sole measure of the extent of initial binding of PLA2 to zwitterionic vesicles or monolayers.

To recapitulate, immeasurably low rates for the hydrolysis of monodisperse phosphatidylcholines through a monodisperse ES complex of PLA2 provide a basis for identifying, comparing, and contrasting the structural changes that lead to a catalytically competent enzyme at the interface through K_S* and k_{cat}* activation. We believe that the protocols developed in this paper are generally useful for designing suitable assay conditions for interfacial enzymes where the microscopic steady-state condition is satisfied. The analytical basis for these protocols as developed in Appendix should be generally useful for an appreciation of the trends of the kinetic contribution of interfacial unstirred layers associated with larger surfaces.

APPENDIX

Product Diffusion Delay. In the experiments described in the main text, products are formed on extraneous surfaces of the walls of the reaction vessel or stirrer, and/or in the air−water interface. The observation region is equidistant from the bottom and sides of the vessel, and it is formed by the crossing beams for excitation and emission. Thus, diffusion takes place in approximately cubically symmetric regions which include the observation window (Figure 2). However, diffusion is a volume-filling process (*22*), and diffusion times are determined primarily from volume considerations. Thus, for computational simplicity, we will assume that the regions exhibit spherical symmetry. The reaction vessel with a volume V is considered a sphere with a radius L, where $V = 4\pi L^3/3$. Similarly, the observation region is considered a sphere with a radius R, where $L - R$ is the distance from the walls to the outer edges of the observation region. In this way, the smallest diffusion distance and the total volume are considered as the main determinants for the diffusion time.

In this spherical symmetry, the solution to the diffusion equation can easily be found using standard methods (*23*). A single product with a diffusion constant D that starts at time zero at the outer boundary ($r = L$) will at later times have the density

$$\rho(r,t) = \frac{1}{V}\left(1 + \frac{2}{3}\sum_{n=1}^{\infty}\frac{L\sin(k_n r/L)}{r\sin(k_n)}e^{-k_n^2 Dt/L^2}\right) \quad \text{(A1)}$$

at a distance r from the center. The numbers k_n ($n = 1, 2, 3, \ldots$) are the roots of the equation

$$k_n = \tan(k_n) \quad \text{(A2)}$$

It can easily be seen that the density (eq A1) satisfies the diffusion equation with a reflecting barrier at $r = L$, approaches a δ function at $r = L$ when t goes to zero, and approaches the homogeneous distribution $1/V$ after long periods of time. The average density inside the observation region ($r < R$) can be calculated as

$$\bar{\rho}(t) = \frac{3}{4\pi R^3}\int_0^R 4\pi r^2 \rho(r,t)\,dr = \frac{1}{V}\left[1 + \frac{2}{x^3}\sum_{n=1}^{\infty}\frac{\sin(k_n x) - k_n x\cos(k_n x)}{k_n^2\sin(k_n)}e^{-k_n^2 Dt/L^2}\right] \quad \text{(A3)}$$

where $x = R/L$. The mean time before the distribution of the product has equilibrated across the whole observation region can be defined as

$$\tau_D = V\int_0^\infty t\frac{d\bar{\rho}}{dt}\,dt = \frac{L^2}{10D}\left(1 - \frac{R^2}{L^2}\right) \qquad (A4)$$

This integral can be calculated from eq A3 but more easily by considering the Laplace transform of the solution to the diffusion equation. Thus, if there is a burst of activity at time zero, the average time for the products to reach the observation region is given by eq A4. It can be noted that this estimate is different from the average time it would take to diffuse across the distance $L - R$, which is $\tau = (L-R)^2/2D$. The difference appears because products that have once reached the outer boundary of the observation region can easily diffuse out again.

This is the result for the diffusion delay that will accompany a burst of product released at time zero. If it is assumed that the total number of enzymes that are active at the walls is N_w, that the reaction starts at time zero, and that the number of products released is υ_w per enzyme per unit time, then the average product concentration in the observation region can be calculated as

$$\bar{c}(t) = \upsilon_w N_w\int_0^t \bar{\rho}(t - t')\,dt' = \upsilon_w E_w\left[t - \frac{L^2}{10D}(1 - x^2) - \frac{L^2}{D}\frac{2}{x^3}\sum_{n=1}^{\infty}\frac{\sin(k_n x) - k_n x\cos(k_n x)}{{k_n}^4\sin(k_n)}e^{-k_n^2 Dt/L^2}\right] \qquad (A5)$$

Here E_w ($=N_w/V$) is the total concentration of enzymes that are active at the walls. The sum in eq A5 converges quite rapidly, except for small t, and only a few terms are required to describe the concentration. After long periods of time, the exponentials are all zero and eq A4 simply describes a linear increase over time (see Figure 3) which extrapolates to the diffusion delay time, τ_D, given by eq A4.

The experiment registers the amount of protons that have reached the observation region. Proton diffusion is very fast, with a diffusion constant D_{H^+} of 9.3×10^{-5} cm^2/s (*24*). However, electroneutrality requires that the protons diffuse together with counterions. Most likely, these counterions will be Cl^- with a diffusion constant D_{Cl^-} of 2.0×10^{-5} cm^2/s (*24*). Eventually, the negatively charged fatty acid that is produced in the reaction must also redistribute via diffusion in the reaction vessel, and thereby restore an even distribution of Cl^-. Other ions will also participate and influence the effective diffusion rate of the protons. Ion diffusion in electrolytes is a messy problem, and to a first approximation, we assume that the main diffusing species which determine the effective proton diffusion are H^+ and Cl^-. This gives the effective proton diffusion constant

$$D = \frac{2D_{H^+}D_{Cl^-}}{D_{H^+} + D_{Cl^-}} = 3.3 \times 10^{-5}\ \text{cm}^2/\text{s} \qquad (A6)$$

If the reaction vessel has the volume V of 2 mL, the corresponding spherical region of the same volume will have a radius L of 0.78 cm. If the observation region is 0.24 cm from the walls, $L - R = 0.24$ and the ratio $x = R/L = 0.69$. These numbers give an expected delay time τ_D from eq A4 of 16 min. This is likely to be a lower limit estimate since the diffusion constants are calculated for infinite dilution, and increasing electrolyte concentrations are expected to slow the effective diffusion. On the other hand, τ_D is a mean time before the distribution of product has equilibrated between the observation region and the rest of the volume. On the basis of the burst kinetics described by eq A3, the time it takes to reach 5 or 10% of the equilibrium value for the product amount in the observation region will be 3 or 4 min, respectively, if $R/L = 0.69$. The reaction progress curves without stirring, of the type shown in Figure 3B, exhibit a time delay of between 5 and 10 min depending on the total substrate concentration.

REFERENCES

1. Jain, M. K., Rogers, J., Jahagirdar, D. V., Marecek, J. F., and Ramirez, F. (1986) *Biochim. Biophys. Acta 860*, 435−447.
2. Jain, M. K., Rogers, J., Berg, O., and Gelb, M. H. (1991) *Biochemistry 30*, 7340−7348.
3. Jain, M. K., Gelb, M. H., Rogers, J., and Berg, O. G. (1995) *Methods Enzymol. 249*, 567−614.
4. De Haas, G. H., Bonsen, P. P. M., Pieterson, W. A., and Van Deenen, L. L. M. (1971) *Biochim. Biophys. Acta 239*, 252−266.
5. Verheij, H. M., Slotboom, A. J., and de Haas, G. H. (1981) *Rev. Physiol. Biochem. Pharmacol. 91*, 91−203.
6. Berg, O. G., Rogers, J., Yu, B., Yao, J., Romsted, L. S., and Jain, M. K. (1997) *Biochemistry 36*, 14512−14530.
7. Berg, O. G., Yu, B.-Z., Rogers, J., and Jain, M. K. (1991) *Biochemistry 30*, 7283−7297.
8. Jain, M. K., Yu, B.-Z., and Berg, O. G. (1993) *Biochemistry 32*, 11319−11329.
9. de Haas, G. H., Dijkman, R., Ransac, S., and Verger, R. (1990) *Biochim. Biophys. Acta 1046*, 249−257.
10. Yuan, W., Quinn, D. M., Sigler, P. B., and Gelb, M. H. (1990) *Biochemistry 29*, 6082−6094.
11. Rogers, J., Yu, B. Z., and Jain, M. K. (1992) *Biochemistry 31*, 6056−6062.
12. Jain, M. K., Tao, W., Rogers, J., Arenson, C., Eibl, H., and Yu, B.-Z. (1991) *Biochemistry 30*, 10256−10268.
13. Jain, M. K., Rogers, J., Marecek, J. F., Ramirez, F., and Eibl, H. (1986) *Biochim. Biophys. Acta 860*, 462−474.
14. Jain, M. K., Ranadive, G. N., Yu, B. Z., and Verheij, H. M. (1991) *Biochemistry 30*, 7330−7340.
15. Jain, M. K., Kraus, C. D., Buckley, J. T., Bayburt, T., and Gelb, M. G. (1994) *Biochemistry 33*, 5011−5020.
16. Yu, B.-Z., Berg, O. G., and Jain, M. K. (1993) *Biochemistry 32*, 6485−6492.
17. Yu, B. Z., Ghomashchi, F., Cajal, Y., Annand, R. R., Berg, O. G., Gelb, M. G., and Jain, M. K. (1997) *Biochemistry 36*, 3870−3881.
18. Rogers, J., Yu, B. Z., Tsai, M. D., Berg, O. G., and Jain, M. K. (1998) *Biochemistry 37*, 9549−9556.
19. Pattus, F., Slotboom, A. J., and De Haas, G. H. (1979) *Biochemistry 18*, 2691−2697.
20. Jain, M. K., and Berg, O. G. (1989) *Biochim. Biophys. Acta 1002*, 127−156.
21. Upreti, G. C., and Jain, M. K. (1980) *J. Membr. Biol. 55*, 113−123.
22. Berg, O. G., and Von Hippel, P. H. (1985) *Annu. Rev. Biophys. Biophys. Chem. 14*, 131−160.
23. Carslaw, H. S., and Jaeger, J. C. (1947) *Conduction of Heat in Solids*, Oxford University Press, London.
24. Daniels, F., and Alberty, R. A. (1966) *Physical Chemistry*, 3rd ed., pp 396−407, Wiley, New York.

BI990194Z